DOI 10.5012/bkcs.2010.31.12.3632

Synthesis of Some Novel Pyrimidine Derivatives and Investigation of their Electrochemical Behavior

Esvet Akbas,* Abdulkadir Levent,†,* Selçuk Gümüş, Mehmet Rauf Sümer, and İnci Akyazı

Yuzuncu Yil University, Faculty of Arts and Sciences, Department of Chemistry, 65080. Van, Turkey
**E-mail: esvakbas@hotmail.com*
†Batman University, Faculty of Arts and Sciences, Department of Chemistry, 72100, Batman, Turkey
**E-mail: leventkadir@hotmail.com*
Received August 31, 2010, Accepted October 5, 2010

2-Iminopyrimidines (**1a-e**) and 2-thioxopyrimidine (**2**) were synthesized using the Biginelli three component cyclocondensation reaction of an appropriate β-diketone, arylaldehyde, and guanidine (for **1a-e**) or thiourea (for **2**). The electrochemical properties of the novel systems were investigated by CV and DPV. Moreover, B3LYP/6-31G(d,p) method was applied to the present structures in order to gather some structural and physicochemical data.

Key Words: 2-Iminopyrimidines, 2-Thioxopyrimidine, Biginelli cyclocondensation, Electrochemical properties

Introduction

The pyrimidines have been subjected to a large variety of structural modifications in order to synthesize derivatives with different biological properties. Many substituted pyrimidine rings play an important role as analgesic, antipyretic, antihypertensive and anti-inflammatory drugs also as pesticides, herbicides, plant growth regulators and organic calcium channel modulators.[1-7]

Various synthesis methods have been reported in the literature for pyrimidine derivatives.[1-18] Most of them are based on the simple Biginelli three component cyclocondensation reaction.[19] This is very simple one-pot, acid catalyzed cyclocondensation reaction of benzaldehyde (**I**), urea (**II**) and ethyl acetoacetate (**III**). The reaction was carried out in ethanol with a few drops of concentrated hydrochloric acid and finalized 3,4-dihydropyrimidine-2(1*H*)-one (**IV**) (Scheme 1).[19,20]

Herein, we have reported the synthesis of 2-iminopyrimidines (**1a-e**) and 2-thioxopyrimidine (**2**), *via* the general method of Biginelli cyclocondensation reaction. The electrochemical properties of the novel systems were investigated by CV and DPV. Moreover, B3LYP/6-31G(d,p) method was applied to the present structures in order to gather some structural and physicochemical data.

Experimental

Melting points were determined on an Electrothermal Gallenkamp apparatus and are uncorrected. Microanalyses were performed on LECO CHNS 932 Elemental Analyzer. The IR spectra were obtained in as potassium bromide pellets using a Mattson 1000 FTIR spectrometer. The ^{1}H and ^{13}C NMR spectra were recorded on Varian Mercury 400 MHz spectrometers, using TMS as an internal standard. All experiments were followed by TLC using DC Alufolien Kieselgel 60 F 254 Merck and Camag TLC lamp (254/366 nm). Electrochemical measurements were performed on a BAS 100W electrochemical analyzer (Bioanalytical System, USA) using a three electrode system, glassy carbon working electrode (Φ: 3 mm, BAS), platinum wire as auxiliary electrode and Ag/AgCl (NaCl 3M, Model RE-1, BAS, USA) as reference electrode. The reference electrode was separated from the bulk solution by a fritted-glass bridge filled with the solvent/supporting electrolyte mixture. Before starting each experiment, the glassy carbon electrode was polished manually with alumina (Φ: 0.01 μM). Cyclic voltammetric (CV) and differential pulse voltammetry (DPV) experiments were recorded at room temperature in extra pure dimethyl formamide (DMF), and ionic strength was maintained at 0.1 mol L^{-1} with electrochemical grade tetrabutylammonium perchlorate (TBAP) as the supporting electrolyte. Solutions were deoxygenated by a stream of high purity nitrogen for 15 min prior to the experiments, and during the experiments nitrogen flow was maintained over the solution.

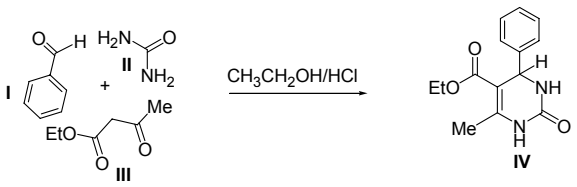

Scheme 1. Synthesis of 3,4-dihydropyrimidine-2(1*H*)-one

General procedure for compounds (1a-d). Guanidine 0.2293 gr (2.4 mmol), dibenzoylmethane 0.4928 gr (2.2 mmol), arylaldehyde (2 mmol) and $NaHCO_3$ 0.67208 gr (8 mmol) were added to DMF (20 mL). This mixture was heated at 70 °C for 5 h. The reaction was cooled to room temperature and poured over crushed ice (25 g). The resulting suspension was filtered off and recrystallized from suitable solvents.

5-Benzoyl-4-(4-chlorophenyl)-6-phenyl-1,2,3,4-tetrahydro-2-iminopyrimidine (1a). $C_{23}H_{18}ClN_3O$, mp 124 - 125 °C. IR (KBr) δ (cm^{-1}) 3345-3138 (NH), 1619 (C=NH), 1595 (C=O). ^{1}H-NMR (400 MHz DMSO-d_6, δ/ppm) δ 10.2 (s, 1H, N_1H), 9.3 (bs, 1H, N_3H), 8.2-7.3 (m, 14H, Ar-H), 4.93-4.91 (d, 1H, C_4H, J = 8.2 Hz). ^{13}C-NMR (DMSO-d_6, δ/ppm) δ 186.0, 176.5, 159.7, 145.1, 141.5, 139.5, 135.3, 133.7, 131.3, 129.9, 129.5, 128.9,

128.1, 127.5, 126.1, 93.9, 52.0. Anal. Calcd.: C, 71.22; H, 4.68; N, 10.83. Found: C, 71.20; H, 4.70; N, 10.80.

5-Benzoyl-4-(3-nitrophenyl)-6-phenyl-1,2,3,4-tetrahydro-2-iminopyrimidine (1b). $C_{23}H_{18}N_4O_3$, mp 110 - 111 °C. IR (KBr) δ (cm^{-1}) 3256 - 3145 (NH), 1623 (C=NH), 1593 (C=O). ^{1}H-NMR (400 MHz DMSO-d_6, δ/ppm) δ 10.6 (s, 1H, N_1H), 9.1 (bs, 1H, N_3H), 8.3-6.9 (m, 14H, Ar-H), 5.09-5.06 (d, 1H, C_4H, J = 11.8 Hz). ^{13}C-NMR (DMSO-d_6, δ/ppm) δ 185.2, 176.6, 159.7, 148.7, 144.9, 143.9, 139.5, 134.6, 131.4, 130.8, 129.4, 129.2, 128.9, 128.4, 126.2, 123.4, 122.5, 80.3, 51.2. Anal. Calcd.: C, 69.34; H, 4.55; N, 14.06. Found: C, 69.38; H, 4.58; N, 14.12.

5-Benzoyl-4-(4-cyanophenyl)-6-phenyl-1,2,3,4-tetrahydro-2-iminopyrimidine (1c). $C_{24}H_{18}N_4O$, mp 207 - 209 °C. IR (KBr): δ (cm^{-1}) 3250-3057 (NH), 2225 (CN), 1675 (C=NH), 1588 (C=O). ^{1}H-NMR (400 MHz DMSO-d_6, δ/ppm) δ 11.1 (s, 1H, N_1H), 9.1 (bs, 1H, N_3H), 8.5-7.3 (m, 14H, Ar-H), 5.1-5.08 (d, 1H, C_4H, J = 8 Hz). ^{13}C-NMR (DMSO-d_6, δ/ppm) δ 198.7, 166.7, 163.9, 159.4, 149.2, 141.3, 137.1, 134.6, 131.4, 130.8, 129.4, 128.9, 128.4, 119.5, 114.1, 110.1, 109.4, 46.8. Mass (100eV): *m/e*: 325.2, 326.2, 377.1, 378.1 (M), 379.1(M+1).

5-Benzoyl-4,6-diphenyl-1,2,3,4-tetrahydro-2-iminopyrimidine (1d). $C_{23}H_{19}N_3O$, mp 149 - 150 °C. IR (KBr): δ (cm^{-1}) 3403-3176 (NH), 1665 (C=NH), 1630(C=O). ^{1}H-NMR (400 MHz DMSO-d_6, δ/ppm) δ 10.2 (bs, 1H, N_1H), 9.3 (bs, 1H, N_3H), 8.1-7.0 (m, 15H, Ar-H), 4.96-4.93 (d, 1H, C_4H, J = 12 Hz). ^{13}C-NMR (DMSO-d_6, δ/ppm) δ 176.5, 163.7, 159.8, 145.1, 141.5, 139.6, 131.3, 131.1, 129.4, 128.9, 128.7, 128.5, 128.3, 127.5, 126.2, 80.3, 51.6. MS (*m/z*) 250.1, 270.1, 321.2, 354.1(M+1).

5-Benzoyl-4-(4-carboxyphenyl)-6-phenyl-1,2,3,4-tetrahydro-2-iminopyrimidine (1e). A mixture of **1c** (1 mmol), 4 mL distilled water, 3 mL CH_3COOH and 3 mL H_2SO_4 was heated at 100 °C for 2 h. The mixture was cooled to room temperature and filtered off. The crude substance was dissolved Na_2CO_3 solition and nötralized H_2SO_4. The resulting suspension was filtered off and recrystallized from acetic acide. $C_{24}H_{19}N_3O_3$. mp > 300 °C. IR (KBr) δ (cm^{-1}) 3451-3329 (NH), 1663 (C=O, acid), 1608 (C=NH), 1576 (C=O, benzoyl). Anal. Calcd.: C, 72.53; H, 4.82; N, 10.57. Found: C, 72.58; H, 4.85; N, 10.52.

5-Benzoyl-6-phenyl-4-(4-hydroxyphenyl)-1,2,3,4-tetrahydro-2-thioxopyrimidine (2). A mixture of dibenzoylmethane (1.6 mmol), 4-hydroxyaldehyde (1.1 mmol), thiourea (1.1 mmol) and 10 mL of glacial acetic acid containing a few drops concentrated hydrochloric acid was heated under reflux for 8 h. The solution was allowed to stand approximately 3 - 4 hours to yield 52 - 65% of product **2**.

$C_{23}H_{18}N_2O_2S$, mp 258 - 259 °C. IR (KBr) δ (cm^{-1}) 3250-3156 (NH), 1601 (C=O), 1270 (C=S). ^{1}H-NMR (400 MHz DMSO-d_6, δ/ppm) δ 10.5 (s, 1H, -OH), 9.7 (d, 1H, N_3H, J = 1.6 Hz), 9.5 (bs, 1H, N_1H), 7.3-6.7(m, 14H, Ar-H), 5.3 (d, 1H, C_4H, J = 4 Hz). ^{13}C-NMR (DMSO-d_6, δ/ppm) δ 195.6, 175.3, 157.7, 144.7, 139.6, 134.1, 133.2, 131.7, 130.5, 129.5, 129.2, 128.5, 128.2, 128.1, 115.9, 111.3, 55.9. Anal. Calcd.: C, 71.48; H, 4.69; N, 7.25. Found: C, 71.50; H, 4.68; N, 7.22.

Results and Discussion

Synthesis of 1a-e and 2. The purpose of the present work was to extend the examples of the Biginelli reactions with the synthesis of some new 2-iminopyrimidine and 2-thioxopyrimidine derivatives.

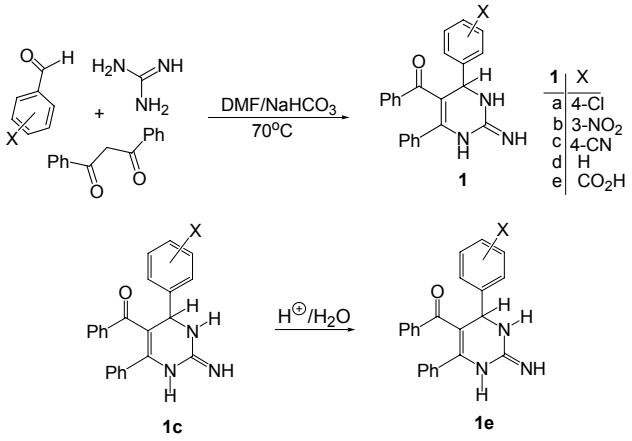

Scheme 2. Synthesis of 2-iminopyrimidines and hydrolysis of **1c**

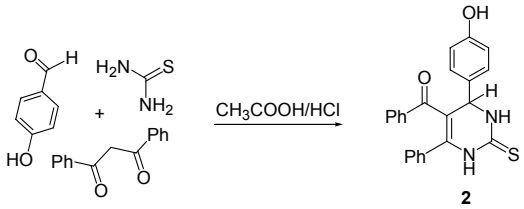

Scheme 3. Synthesis of 2-thioxopyrimidine

The compounds **1a-d** were prepared from the cyclocondensation reaction of dibenzoylmethane, arylaldehydes and guanidine under DMF/$NaHCO_3$ condition at 70 °C (Scheme 2). The condensation of dibenzoylmethane, 4-hydroxyaldehyde, and thiourea in acetic acid, catalyzed by HCl was resulted in the synthesis of 2-thioxopyrimidine (**2**) (Scheme 3). Both reactions proceeded according to the Biginelli reaction.[19]

All compounds were characterized on the basis of their spectral data and elementary analyses or MS. The IR spectra of the pyrimidine compounds displayed absorption bands characteristic for the NH stretching at 3451 - 3057 cm^{-1} and C=O stretching at 1675 - 1588 cm^{-1}, and showed C=S function at 1270 cm^{-1} for compound **2**.

In ^{1}H NMR spectra, the formation of the pyrimidine ring in this reaction was clearly demonstrated by the fact that the C_4 methine proton of all compounds appeared at 5.4 - 4.9 ppm as doublet. The signals of the N_3H and N_1H protons of the compounds appeared one proton singlets at 11.1 - 10.2 and 10.3 - 9.1 ppm, respectively. The signals of the other protons were appeared at the expected chemical shifts and integral values (see experimental).

The 4-carboxyphenyl, 2-iminopyrimidine (**1e**) was prepared *via* hydrolysis of compound 4-cyanophenyl, 2-iminopyrimidine (**1c**) (Scheme 2). In the IR spectra of compound **1e**, the absence of the characteristic absorption band at 2225 cm^{-1} of the CN group of the starting material (**1c**) was a good evidence of the expected reaction. Meanwhile, the corrosion inhibitor properties of the compound **1e** were studied by our group.[21]

Electrochemical analysis. The electrochemical properties

of the present compounds were investigated by CV and DPV on a glassy carbon electrode in DMF containing 0.1 M TBAP, in the concentration of 1×10^{-3} M *vs*. Ag/AgCl. The electrochemical data upon the peak potentials have been reported in Table 1.

In the cathodic direction from +1.4 V to −2.5 V at scan rate of 100 mV s^{-1}, the CV and DPV of **1a** is characterized by five cathodic waves (Ic, IIc, IIIc, IVc and Vc at about −1.14, −1.45, −1.61, −1.95 and −2.29 V, respectively) and two anodic waves (IIa and IVa at about −1.30 and −1.77 V, respectively) as depicted by cyclic voltammograms given in Figure 1. DPV of **1a** confirms also the recorded redox processes clearly (Figure 1). At higher scan rates (≥ 100 mV s^{-1}) a new redox couple was observed (I′c/I′a), which located at potentials ranging from +0.24 to +0.29 V (Figure 4). The peak separation (ΔE_p) was also found to be 50 mV which indicates a reversible electron transfer in the electrode reaction.

The electrochemical behavior of the **1b** is presented in Figure 1. In the CV measurements upon scanning cathodically at the negative potential side (from +1.4 to −2.5 V at 100 mV s^{-1}), the CV and DPV of **1b** is characterized by three cathodic waves (Ic, IIc, and IIIc at about −1.05, −1.50 and −1.99 V, respectively) and with their anodic partners (Ia, IIa and IIIa at about −0.94, −1.33 and −1.59 V, respectively). ΔE_p for this redox couples (Ia/Ic, IIa/IIc and IIIa/IIIc) were also found to be 110, 170 and 400 mV, respectively. These data indicate that quasi-reversible electron transfer occurs in the electrode reaction. At higher scan rates (≥ 250 mV s^{-1}) the redox process showed a new reversible redox couple (I′c/I′a) located at potentials ranging from −0.74 to −0.70 V, also two anodic waves were located at about −0.38 and +0.16 V (Figure 4). ΔE_p for this redox couples (Ia/Ic and IIa/IIc) were also found to be 90 and 120 mV, respectively. It indicates a quasi-reversible electron transfer in the electrode reaction.

The voltammograms of **1c** compound investigated in the same experimental conditions (from +1.4 V to −2.5 V at 100 mV s^{-1} in Figure 2). three cathodic waves (Ic, IIc, and IIIc at about −1.36, −1.62 and −1.89 V, respectively) and two anodic waves

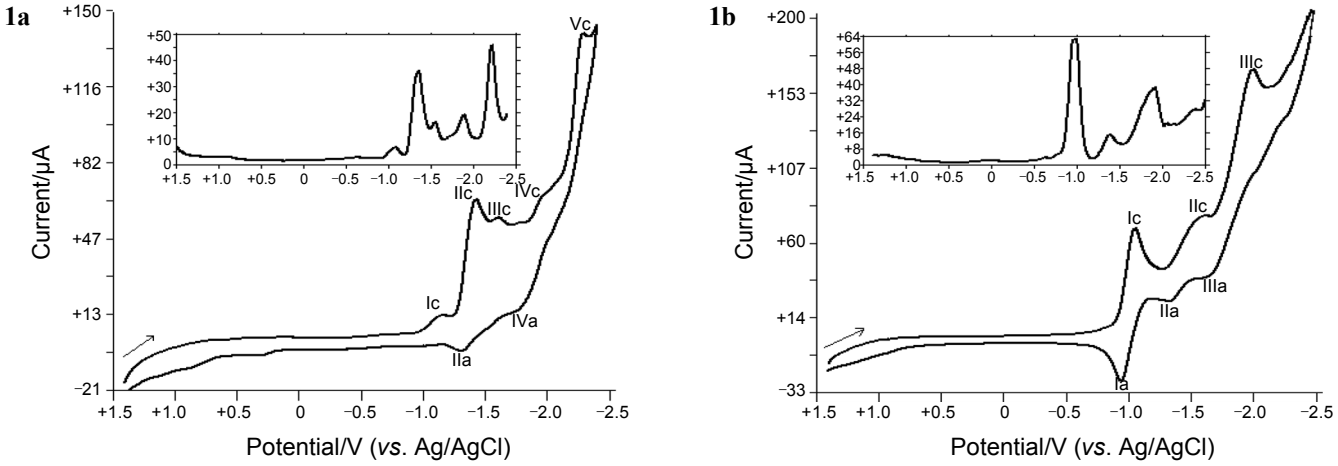

Figure 1. Cyclic voltammogram of **1a** and **1b** compounds (1×10^{-3} M) at 0.100 Vs^{-1} scan rate on glassy carbon electrode in DMF/TBAP. Insert: differential pulse voltammogram (DPV) of **1a** and **1b** compounds (1×10^{-3} M). DPV parameters; Pulse amplitude: 50 mV, sample width = 17 ms, Pulse width = 50 ms, pulse period = 200 ms and scan rate = 20 mV s^{-1}.

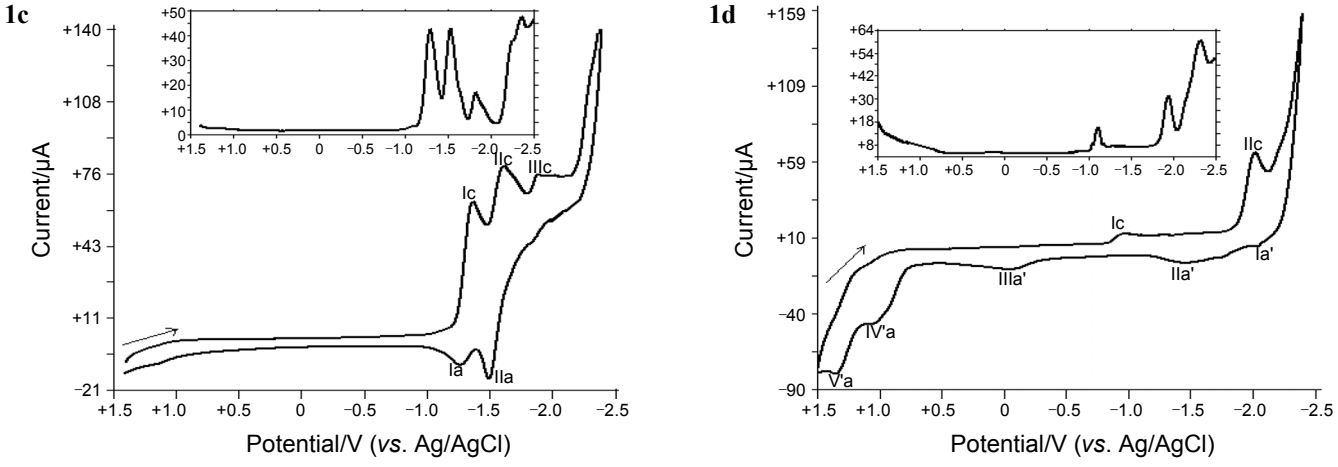

Figure 2. Cyclic voltammogram of **1c** and **1d** compounds (1×10^{-3} M) at 0.100 Vs^{-1} scan rate on glassy carbon electrode in DMF/TBAP. Insert: DPV of **1c** and **1d** compounds (1×10^{-3} M). DPV parameters as indicated in Figure 1.

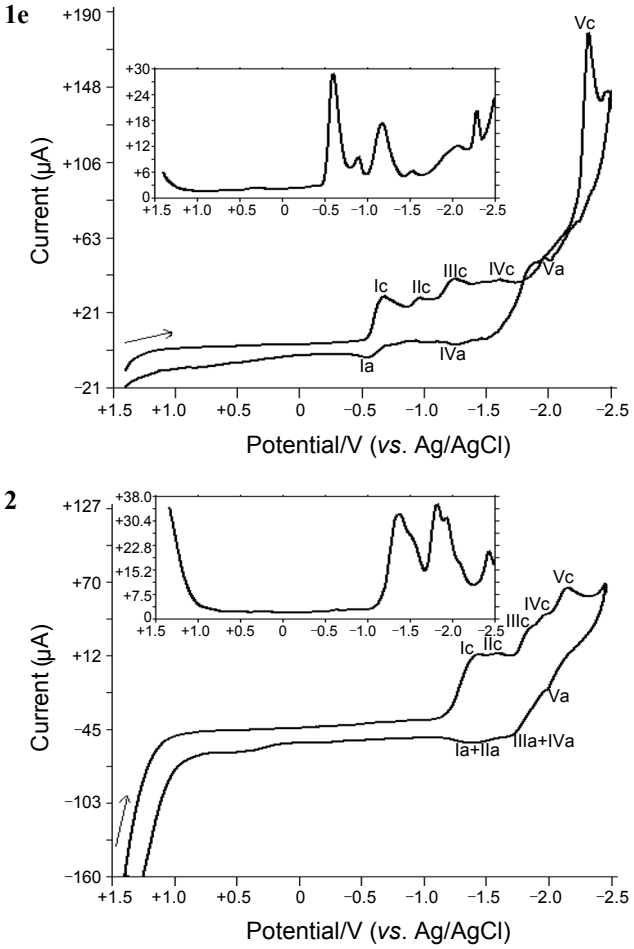

Figure 3. Cyclic voltammogram of **1e** and **2** compounds (1×10^{-3} M) at 0.100 Vs^{-1} scan rate on glassy carbon electrode in DMF/TBAP. Insert: DPV of **1e** and **2** compounds (1×10^{-3} M). DPV parameters as indicated in Figure 1.

(IIa and IVa at about −1.27 and −1.50, respectively) were observed, DPV of **1c** confirms also the recorded redox processes clearly (Figure 2). At higher scan rates (≥ 500 mV s^{-1}) the redox process was observed a new irreversible cathodic wave located at potentials +0.46 V (Figure 4).

In the cathodic direction from +1.4 V to −2.5 V at scan rate of 100 mV s^{-1}, the CV and DPV of **1d** is characterized by two cathodic waves (Ic and IIc at about −0.92 and −2.02 V, respectively) and five anodic waves (Ia', IIa' IIIa', IVa' and Va' at about −2.05, −1.47, +0.04, +1.05 and +1.35 V, respectively) as depicted by cyclic voltammograms given in Figure 2. DPV of **1d** confirms the recorded redox processes (for higher scan rates at ≥ 250 mV s^{-1}) clearly (Figure 2). These peaks are irreversible. At higher scan rates (≥ 500 mV s^{-1}) the redox process was observed two new irreversible cathodic waves located at potentials −1.33 and −1.62 V (Figure 5).

The electrochemical behavior of the **1e** is presented in Fig. 3. The CV measurements were obtained upon scanning cathodically at the negative potential side from +1.4 to −2.5 V at 100 mV s^{-1}. The CV and DPV of **1e** are characterized by three cathodic waves (Ic, IIc, IIIc, IVc and Vc at about −0.68, −0.96, −1.24, −1.61 and −2.32 V, respectively) and with their anodic partners

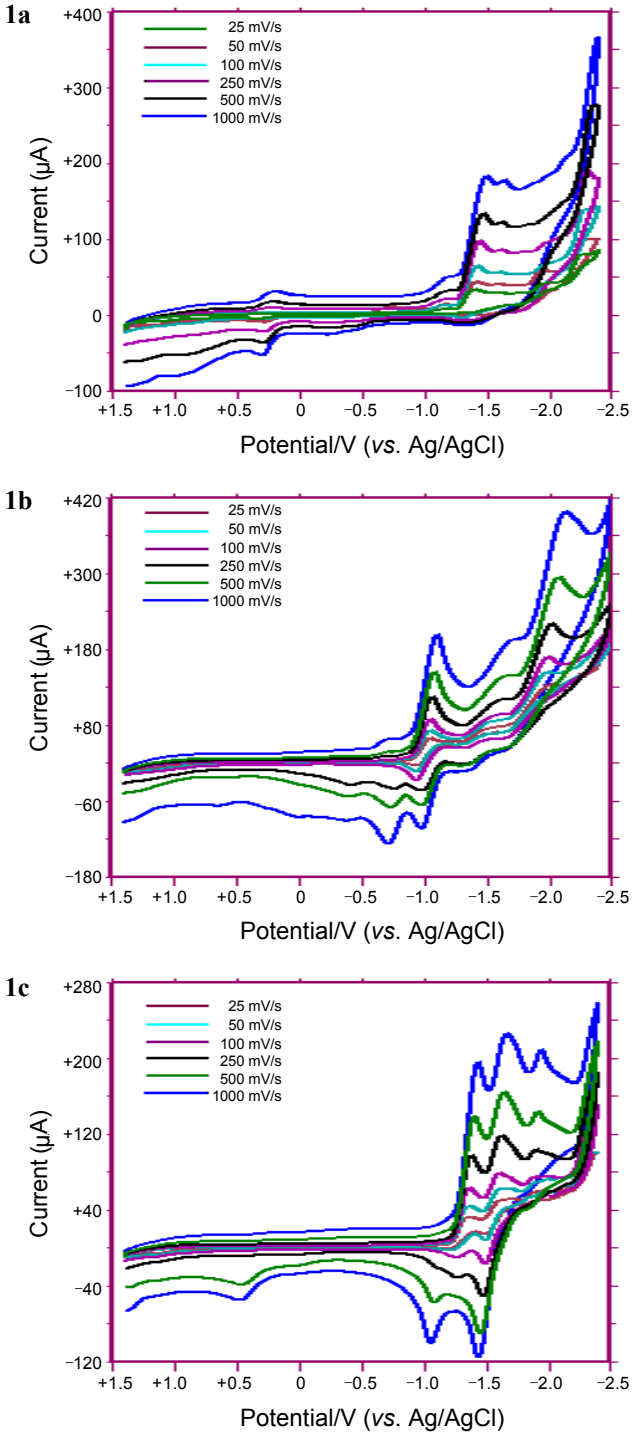

Figure 4. Cyclic voltammograms of **1a**, **1b** and **1c** compounds (1×10^{-3} M) at on glassy carbon electrode in DMF/TBAP at various scan rates.

(Ia, IVa and Va at about −0.56, −1.27 and −2.02 V, respectively). When the potential sweep was reversed before IIc (at *ca.* −0.85 V) and Vc (at *ca.* −1.77 V), Ia and IVa oxidation steps were produced. ΔE_p for this redox couples (Ia/Ic, IVa/IVc and Va/Vc) were also found to be 120, 340 and 300 mV, respectively. These data imply that quasi-reversible electron transfer occurs in the electrode reaction. At higher scan rates (≥ 500 mV s^{-1}) the redox process was showed a new irreversible anodic wave located at

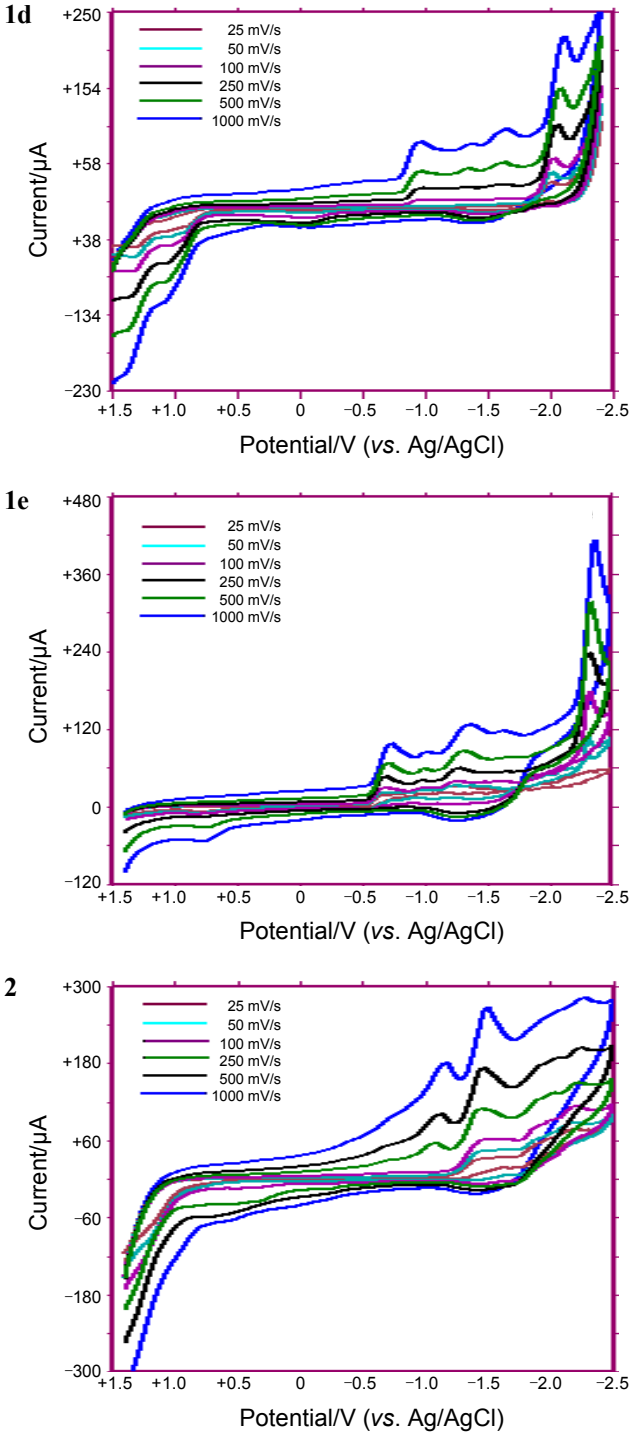

Figure 5. Cyclic voltammograms of **1d**, **1e** and **2** compounds (1×10^{-3} M) at on glassy carbon electrode in DMF/TBAP at various scan rates.

potentials +0.76 V (Figure 5).

In the cathodic direction from +1.4 V to −2.5 V at scan rate of 100 mV s^{-1}, the CV and DPV of **2** are characterized by five cathodic waves (Ic, IIc, IIIc, IVc and Vc at about −1.48, −1.64, −1.88, −2.02 and −2.19 V, respectively) and three anodic waves (Ia+IIa, IIIa+IVa and Va at about −1.42, −1.75 and −2.04 V, respectively) as depicted by cyclic voltammograms given in Figure 3, which is also confirmed by the recorded redox process-

Table 1. Voltammetric results in V *vs* Ag/AgCl. Scan rate, 100 mV s^{-1}. *E*c: cathodic, *E*a: anodic.

Compound	*Ec*	*Ea*
1a	**Ic:** −1.14, **IIc:** −1.45, **IIIc:** −1.61, **IVc:** −1.95, **Vc:** −2.29	**IIa:** −1.30, **IVa:** −1.77
1b	**Ic:** −1.05, **IIc:** −1.50, **IIIc:** −1.99	**Ia**: −0.94, **IIa:** −1.33, **IIIa:** −1.59
1c	**Ic:** −1.36, **IIc:** −1.62, **IIIc:** −1.89	**Ia**: −1.27, **IIa:** −1.50
1d	**Ic:** −0.92, **IIc:** −2.02	**Ia'**: −2.05, **IIa':** −1.47, **IIIa':** +0.04, **IVa':** +1.05, **Va':** +1.35
1e	**Ic:** −0.68, **IIc:** −0.96, **IIIc:** −1.24, **IVc:** −1.61, **Vc:** −2.32	**Ia:** −0.56, **IVa:** −1.27, **Va:** −2.02
2	**Ic:** −1.48, **IIc:** −1.64, **IIIc:** −1.88, **IVc:** −2.02, **Vc:** −2.19	**Ia+IIa:** −1.42, **IIIa+IVa:** −1.75, **Va:** −2.04

es by DPV of **2** (Figure 3). At higher scan rates (≥ 250 mV s^{-1}) a new redox wave was observed located at potential −1.05 V, and Ic and IIc cathodic waves were turned a new wave located at potential −1.46 V (Figure 5).

Taking into account the reported data concerning electrochemical behavior of recently synthesized pyrimidine compounds such as 1-amino-5-benzoyl-4 phenyl-1H-pyrimidine-2-one[22] and *N*-(5-benzoyl-2-oxo-4-phenyl-2H-pyrimidin-1-yl)-oxalamic acid or malonamic acid[21,23,24] at hanging mercury drop and glassy carbon electrodes, respectively, the electron-donating groups lower the oxidation potentials, while electron-withdrawing groups have the opposite effect.[25] In each series of compounds, the cathodic peak potential corresponding to the intramolecular reductive coupling of the imine and carbonyl groups varies as can be expected from the electronic effects of the substituents attached to the phenyl bounded at position 4 of the dihydropyrimidine ring system. Thus, in the present case, the cathodic peak potential becomes more negative according to the sequence NO_2, CN, COOH and Cl, in order of an decrease in both electron-withdrawing and acceptor qualities of the substituents. On the other hand, the location of an electron donating OH group on the phenyl connected to C_4, together with the replacement of the imine with thioxo moiety in the case of compound **2** results in even much negative electron potentials. This agrees with a mechanism involving self-protonation reactions for the electrochemical reduction of the imine or thio, and carbonyl groups in pyrimidines in the present study.

Computational analysis. The present systems **1a-e** and **2** were subjected to theoretical analysis in order to obtain some structural and physicochemical data.

The initial geometry optimizations of the dihydropyridine derivatives leading to energy minima were achieved by using MM2 method followed by semi-empirical PM3 self-consistent fields molecular orbital (SCF MO) method[26,27] at the restricted level.[28] Then, final geometry optimizations were performed within the framework of density functional theory (DFT, B3LYP)[29,30] at the level of 6-31G(d,p) (restricted closed-shell)

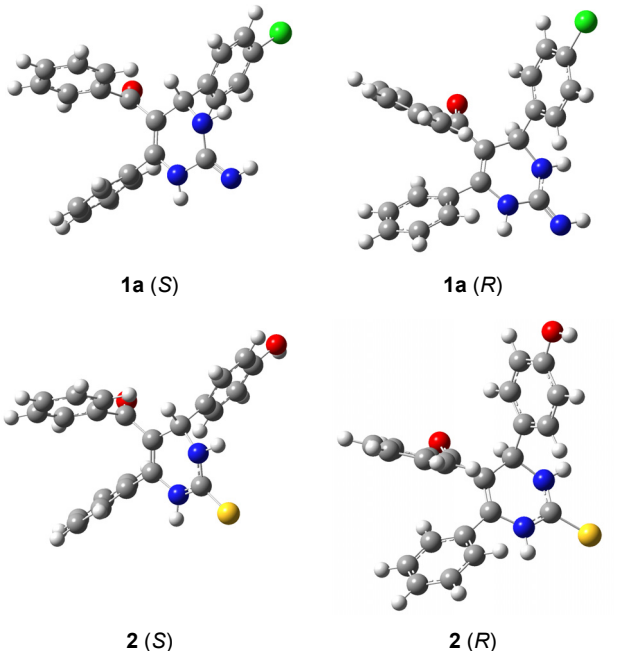

Figure 6. The geometry optimized structures of **1a** and **2** (B3LYP/6-31G(d,p)).

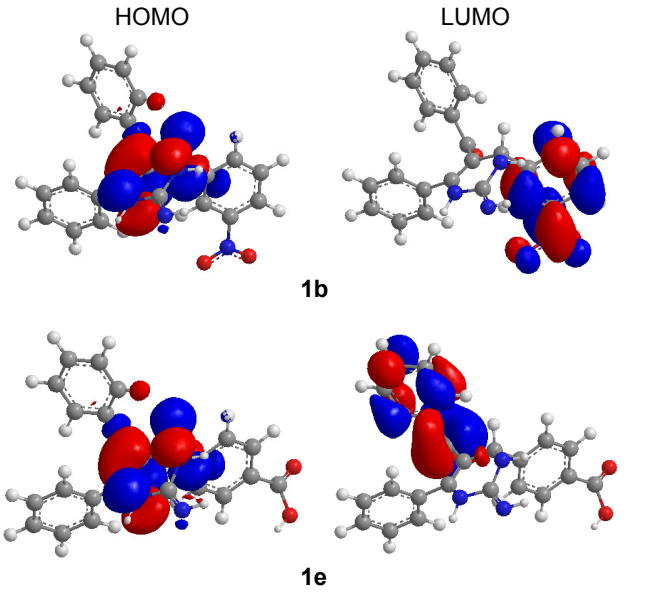

Figure 7. 3D HOMO and LUMO molecular orbital schemes of **1b** and **1e**.

without any geometrical restriction. The exchange term of B3LYP consists of hybrid Hartree-Fock and local spin density (LSD) exchange functions with Becke's gradient correlation to LSD exchange.[31] The correlation term of B3LYP consists of the Vosko, Wilk, Nusair (VWN3) local correlation functional[32] and Lee, Yang, Parr (LYP) correlation correction functional.[33] The BLYP method gives a better improvement over the SCF-HF results. Its predictions are in qualitative agreement with experiment.[34-36] The normal mode analysis for each structure yielded no imaginary frequencies for the 3*N*-6 vibrational degrees of freedom, where *N* is the number of atoms in the system. This indicates that the structure of each molecule corresponds to at least a local minimum on the potential energy surface.

All these computations have been performed using Gaussian 03 package programe.[37]

The geometry optimized structures of **1a** and **2** have been given in Figure 6. It should be noted that there exist a stereogenic center at C_4 carbon. The total energies of the R and S differs from each other with an average of 8 kJ/mol in favor of the S enantiomer. The better stability of *S* over *R* can be explained by the decrease in the steric crowdness of the three phenyl moieties of the system in the case of the S enantiomer.

The calculated total energies (zero point corrected), frontier molecular orbital energies (HOMO and LUMO) and interfrontier energy gap data have been given in Table 2. The data in this table reveal that the HOMO values in the cases of **1b**, **1c**, **1e** (when stronger electron withdrawing groups are attached to the phenyl attached to C_4) are greater in absolute value than the other derivatives. Whereas, higher HOMO levels have been obtained for the other cases (**1a**, **1d**, **2**), that is, when the phenyl group possesses relatively more electron donating groups. On the other hand, LUMO energy for **1d** (X=H) is the highest among all while lowest for **1b** (X=NO_2, $\varepsilon_{LUMO} = -2.80$ eV). As a result, the nitro

Table 2. The computed total energies (Hartrees), and frontier molecular orbital energies (eV) of the synthesized compounds.

Compound	Total Energy		HOMO	LUMO	Δε
	S	*R*			
1a	−1587.6526756	−1587.6499709	−5.88	−1.85	4.04
1b	−1332.5005211	−1332.4945199	−6.01	−2.80	3.21
1c	−1220.2894354	−1220.2859317	−6.02	−1.95	4.06
1d	−1128.0779987	−1128.0740767	−5.70	−1.70	4.00
1e	−1316.5725190	−1316.5680041	−6.03	−1.98	4.05
2	−1546.1211019	−1546.1194646	−5.72	−2.13	3.59

derivative has been found to be more reactive on nucleophilic attack. The relatively lower LUMO energy value (−2.13 eV) for thioxo derivative is thought to be due to the electron donating effect of OH substitution on the phenyl ring and the existance of the thioxo moiety. As a consequence of the much lower LUMO levels, **1b** and **2** possess the narrowest HOMO-LUMO gaps (Δε) which will cause readily photo-induced excitation that may lead subsequent chemical reactions.

The 3D HOMO and LUMO molecular orbital schemes of **1b** and **1e** are shown in Figure 7. The HOMO for all systems is mostly composed of the nitrogens of the central ring with no exceptions, whereas the LUMO is located on the benzoyl part of the systems with **1b** as an exception where the LUMO of the system is located on the nitro substituted phenyl ring.

Conclusion

In conclusion, the synthesis of six novel dihydropyrimidine derivatives has been achieved *via* an application of the one-pot three component Biginelli condensation procedure. The structures of the new compounds have been confirmed by spectroscopic data analysis.

The electrochemical analysis of the present systems showed that the electronic effects of the substituents attached to the phenyl bounded at position 4 of the dihydropyrimidine ring system has a quite important role in the cathodic peak potential corresponding to the intramolecular reductive coupling of the imine and carbonyl groups as expected. The data revealed that the more the electronegative the group attached to the phenyl moiety, the more negative the cathodic peak potential is.

The theoretical calculations reveal parallel results with the outcomes of electrochemical analysis such that, the nitro derivative possesses the lowest LUMO energy resulting in the narrowest Δε gap among the series. Therefore, the compound can be subjected to both oxidative and reductive reactions easier than the other derivatives.

References

1. Alagarsamy, V.; Shankar, D.; Meena, S.; Thirumurugan, K.; Durai Ananda Kumar, T. *Drug Development Research* **2007**, *68*, 134.
2. Sondhi, S. M.; Singh, N.; Johara, M.; Kumarb, A. *Bioorganic & Medicinal Chemistry* **2005**, *13*, 6158.
3. Bruno, O.; Brullo, C.; Ranise, A.; Schenone, S.; Bondavalli, F.; Barocelli, E.; Ballabeni, V.; Chiavarini, M.; Tognolini, M.; Impicciatore, M. *Bioorganic & Medicinal Chemistry Letters* **2001**, *11*, 1397.
4. Nega, S.; Aionso, J.; Diazj, A.; Junquere, F. *J. Heterocycl. Chem.* **1990**, *27*, 269.
5. Shishoo, C. J.; Jain, K. S. *J. Heterocycl. Chem.* **1992**, *29*, 883.
6. Kappe, C. O. *Molecules.* **1998**, *3*, 1.
7. Pathak, P.; Kaur, R.; Kaur, B. *Arkivoc* **2006** (xvi), 160.
8. Yarım, M.; Saraç, S.; Kılıç, F. S.; Erol, K. *II Farmako.* **2003**, 17.
9. Elgazzar, A. B. A.; Gafaar, A. M.; Hafez, H. N.; Aly, A. S. *Phosphorus, Sulfur, and Silicon* **2006**, *181*,1859.
10. Xu, J. M.; Yao, S. P.; Wu, W. B.; Lv, D. S.; Lin, X. F. *J. Molecular Catalysis B: Enzymatic* **2005**, *35*, 122.
11. Eynde, J. J. V; Hecq, N.; Kataeva, O.; Kappe, C. O. *Tetrahedron* **2001**, *57*, 1785.
12. Kappe, C. O.; Roschger, P. *J. Heterocyclic Chem.* **1989**, *26*, 55.
13. Ahmed, E. Kh.; Ameen, M. A.; Abdel-latif, F. F. *Phosphorus*, *Sulfur*, *and Silicon* **2006**, *181*, 497.
14. Mobinikhaledi, A.; Forughifar, N.; Goodarzi, F. *Phosphorus, Sulfur*, *and Silicon and the Related Elements* **2003**, *178*, 2539.
15. Aly, A. A. *Phosphorus*, *Sulfur*, *and Silicon and the Related Elements* **2006**, *181*, 1285.
16. Aslanoğlu, F.; Akbaş, E.; Sönmez, M.; Anıl, B. *Phosphorus*, *Sulfur*, *and Silicon and the Related Elements* **2007**, *182*, 1589.
17. Akbaş, E.; Aslanoğlu, F. *Phosphorus, Sulfur, and Silicon and the Related Elements* **2008**, *183*, 82-89.
18. Akbaş, E.; Aslanoğlu, F; Anıl, B.; Şener, A. *J. Heterocyclic Chem.* **2008**, *45*, 1457.
19. Biginelli, P. *Gazz. Chim. Ital.* **1893**, *23*, 360.
20. Falsone, F. S.; Kappe, C. O. *Arkivoc* **2001**, (ii), 122.
21. a) Caliskan, N.; Akbas, E. "Corrosion inhibition of austenitic stainless steel by some pyrimidine compounds in hydrochloric acid" *Materials and Corrosion* **2010** (Accepted publication). b) Sümer, M. R. *Master Thesis*, Yuzuncu Yil University, FBE Van, Turkey, 2010.
22. Kılıç, H.; Berkem, M. *J. Serb. Chem. Soc.* **2004**, *69*, 689
23. Sönmez, M.; Çelebi, M.; Levent, A.; Berber, İ.; Şentürk. Z. *J. Coord. Chem.* **2010** (in press). (DOI: 10.1080/00958972.2010.494252).
24. Sönmez, M.; Çelebi, M.; Levent, A.; Berber, İ.; Şentürk, Z. *J. Coord. Chem.* **2010**, *63*, 848.
25. Cai, T.; Xian, M.; Wang, P. G. *Bioorganic & MedicinalChemistry Letters* **2002**, *12*, 1507-1510.
26. Stewart, J. J. P. *J. Comput Chem.* **1989**, *10*, 209.
27. Stewart, J. J. P. *J. Comput Chem*. **1989**, *10*, 221.
28. Leach, A. R. *Molecular Modelling, Longman: Essex* **1997**.
29. Kohn, W.; Sham, L. *J. Phys. Rev.* **1965**, *140*, 1133.
30. Parr, R. G.; Yang, W. *Density Functional Theory of Atoms and Molecules*; Oxford University Press: London, 1989.
31. Becke, A. D. *Phys. Rev. A* **1988**, *38*, 3098.
32. Vosko, S. H.; Vilk, L.; Nusair, M. *Can. J. Phys.* **1980**, *58*, 1200.
33. Lee, C.; Yang, W.; Parr, R. G. *Phys. Rev. B* **1988**, *37*, 785.
34. Scuseria, G. E. J. *Chem. Phys.* **1992**, *97*, 7528.
35. Sosa, C.; Lee, C. J. *Chem. Phys.* **1993**, *98*, 8004.
36. Wilson, P. J.; Amos, R. D.; Handy, N. C. *Phys. Chem.* **2000**, *2*, 187.
37. Frisch, M. J.; Trucks, G. W.; Schlegel, H. B.; Scuseria, G. E.; Robb, M. A.; Cheeseman, J. R.; Montgomery, J. A., Jr.; Vreven, T.; Kudin, K. N.; Burant, J. C.; Millam, J. M.; Iyengar, S. S.; Tomasi, J.; Barone, V.; Mennucci, B.; Cossi, M.; Scalmani, G.; Rega, N.; Petersson, G. A.; Nakatsuji, H.; Hada, M.; Ehara, M.; Toyota, K.; Fukuda, R.; Hasegawa, J.; Ishida, M.; Nakajima, T.; Honda, Y.; Kitao, O.; Nakai, H.; Klene, M.; Li, X.; Knox, J. E.; Hratchian, H. P.; Cross, J. B.; Adamo, C.; Jaramillo, J.; Gomperts, R.; Stratmann, R. E.; Yazyev, O.; Austin, A. J.; Cammi, R.; Pomelli, C.; Ochterski, J. W.; Ayala, P. Y.; Morokuma, K.; Voth, G. A.; Salvador, P.; Dannenberg, J. J.; Zakrzewski, V. G.; Dapprich, S.; Daniels, A. D.; Strain, M. C.; Farkas, O.; Malick, D. K.; Rabuck, A. D.; Raghavachari, K.; Foresman, J. B.; Ortiz, J. V.; Cui, Q.; Baboul, A. G.; Clifford, S.; Cioslowski, J.; Stefanov, B. B.; Liu, G.; Liashenko, A.; Piskorz, P. I.; Komaromi, R. L.; Martin, D. J.; Fox, T.; Keith, M. A.; Al-Laham, C. Y.; Peng, A.; Nanayakkara, M.; Challacombe, P. M. W.; Gill, B.; Johnson, W.; Chen, M. W.; Wong, C.; Gonzalez, J. A. *Pople*, *Gaussian 03*, *Gaussian Inc*., *Wallingford*, *CT*, 2004.